



Numerical Simulation on the Reflection Characterisation and Performance of a Solar Collector - A Case Study of UPM Solar Bowl

Ng, K. M.^{1,3*}, Adam, N. M.² and Azmi, B. Z.¹

¹*Alternative and Renewable Energy Laboratory, Institute of Advanced Technology, Universiti Putra Malaysia, 43400 Serdang, Selangor, Malaysia*

²*Department of Mechanical and Manufacturing Engineering, Faculty of Engineering, Universiti Putra Malaysia, 43400 Serdang, Selangor, Malaysia*

³*Department of Mechanical and Automotive Engineering, School of Engineering and Technology Infrastructure, Kuala Lumpur Infrastructure University College, 43000 Kajang, Selangor, Malaysia*

ABSTRACT

A numerical simulation of UPM Solar Bowl is presented in this paper. The numerical analysis considered a general model of solar bowl, which was divided into three modules: (a) reflection characterisation of the bowl, (b) solar flux density along the receiver, and (c) radiation contour mapping of the receiver. The governing equations are resolved in a segregated manner using Matlab programming environment. The influence of the tropical clear sky irradiance on the collector was numerically studied, whereas the collector performance in time domain was also quantified. Single reflection is a major element in thermal concentration. It was observed that solar flux density of collector substantially deteriorated during off solar noon hour, in which during 08:00 and 16:00 under clear sky of tropics, the percentage reduction of flux density is over 82% at all points of the receiver. The simulated radiation contour mapping of the receiver supports the finding. Other results of the UPM Solar Bowl simulation model are also shown and discussed.

Keywords: numerical simulation, reflection characterisation, collector performance, time domain, UPM Solar Bowl

Article history:

Received: 6 December 2010

Accepted: 30 May 2011

Email addresses:

mun_311@hotmail.com (Ng, K. M.),

mariah@eng.upm.edu.my (Adam, N. M.),

azmizak@fsas.upm.edu.my (Azmi, B. Z.)

*Corresponding Author

INTRODUCTION

UPM Solar Bowl is a kind of fixed mirror distributed focus (FMDF) solar collector, which was designed to collect solar energy for power generation purposes. It was constructed at Universiti Putra Malaysia in 1997 as a pioneer solar bowl in Malaysia

(Sulaiman *et al.*, 1997). This system consists of a large and stationary spherical bowl that serves to reflect and focus incident sunrays on a sun tracking linear solar receiver. In addition, a similar solar concentrator was also developed and has been operated since 1980s at Crosbyton, Texas as a research and test facility to investigate its operation components (O'Hair & Green, 1990, 1992). It was a solar thermal power plant employing a steam driven turbine generator as a solar power conversion system (Bethea *et al.*, 1981).

Several studies have been conducted to investigate solar bowl technology. Kreider (1975) presented the thermal performance evaluation of the collector by incorporating the effects of mirror reflectance, concentration ratio, insolation level, fluid flow rate, envelope evacuation and incidence angle in the analysis. Clausing (1976) presented an analytical study for the FMDF collector to evaluate the collector system efficiency. Gandhe *et al.* (1989) fabricated a spherical reflecting bowl to analyse the heat transfer feature of the absorber and the results agreed well with the prediction from mathematical models. Variations of optical concentration for oblique incident rays striking the reflector had also been investigated in another study of Gandhe *et al.* (1986a) who showed that the optical concentration and the surface temperature of absorber decreased with the increment of solar zenith angle. The researchers also presented an optical analysis of a cylindrical absorber and showed the effect of optical concentration on absorber with and without glass cover (Gandhe *et al.*, 1986b). El-Refaie (1989) studied a mathematical model to determine the concentration profiles along the receiver under different conditions. The effects of the reflector rim angle, absorber-to-reflector diameter ratio and multi-reflection zones on the collector are discussed.

Sulaiman *et al.* (1997) have presented a conceptual design of hybrid thermal and photovoltaic receiver for FMDF solar concentrator to harvest solar energy. A solar tracking mechanism of UPM Solar Bowl was designed and demonstrated in both active and passive means (Sulaiman *et al.*, 2008). Similarly, O'Hair and Green (1992) discussed and compared the component efficiencies developed by Battelle laboratory with the actual efficiency factors of solar bowl. Their analysis generated a good agreement between these efficiencies. Dirks *et al.* (1992) presented the performance and cost analysis of a FMDF device to study its reliability in solar energy application. In particular, they studied the efficiency factors that could influence the performance of the collector. The factors involved are cosine losses, shadowing, blocking, reflectivity, atmosphere attenuation, and spillage.

From the previous literature, there are numerous studies presented on the collector performance. However, there is very little investigation conducted on the performance of solar bowl on specific local point of receiver in daytime basis, which is essential to allow utilisation of solar energy collection. Meanwhile, several studies have shown the analysis of reflection and performance characteristics of collector that is limited to solar noon (El-Refaie, 1989; Sulaiman *et al.*, 1997). Although some authors have presented the investigation of collector beyond solar noon (Gandhe *et al.*, 1989; Dicks *et al.*, 1992), there is a need to highlight the information for UPM Solar Bowl that is situated under tropical zone.

In this paper, a detailed numerical simulation of the UPM Solar Bowl is presented on daytime basis. The reflection behaviour, interception of solar irradiation, solar power concentration performance and solar contour mapping of the receiver are resolved iteratively by segregated method on Matlab platform. An average local concentration equation and its

respective boundary condition in accordance with different solar hour are introduced in the model. Then, a simulated clear sky solar irradiance at UPM Solar Bowl is associated in the numerical model to predict its overall solar flux concentration along the receiver in time domain. The simulated results are presented and discussed in the present work.

MODEL DESCRIPTION AND MATHEMATICAL FORMULATION

The simulation model was developed following the features of UPM Solar Bowl which is located at $2^{\circ} 59' N$ $101^{\circ} 42' E$ and an elevation of 59 m. Fig.1 displays the plant. Meanwhile, the parameters of the collector layout are listed in Table 1.

Table 1: The basic physical parameters of UPM Solar Bowl

Parameter	Value
Rim angle (degree)	60
Radius of curvature of solar reflector (m)	27.9
Aperture diameter (m)	48
Receiver-to-collector diameter ratio, R (dimensionless)	0.015

In this study, a mathematical model was developed to simulate the system. Nonetheless, the theoretical approach is not able to consider all reality aspects, and thus, simplification and assumption were done to achieve an approximate solution from the theoretical derivation. The assumptions are: (i) mirror surfaces have ideal spherical curvature, (ii) surface of the reflector is reflecting specularly, (iii) shape of the collector surface is constant, and (iv) tracking error of the receiver within an acceptable range that can be ignored (Garcia-Valladares & Velazquez, 2009).

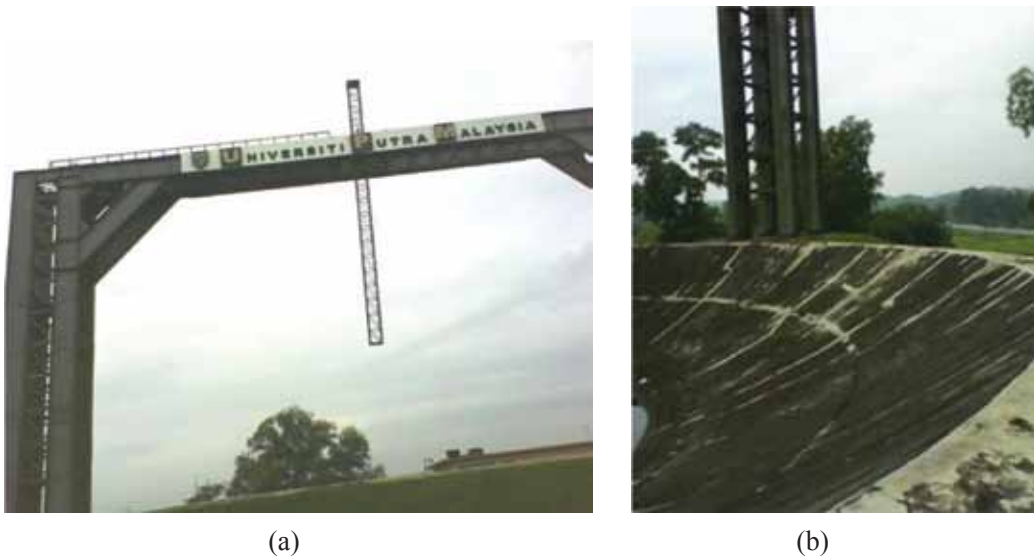


Fig. 1: (a) UPM Solar Bowl at Universiti Putra Malaysia; (b) Spherical curvature of the UPM Solar Bowl

Reflection Characterisation of the Reflector Model

Optical characteristics of a spherical reflector are characterised by the reflector rim angle and the angle of incoming sunrays on the reflector. The degree of reflection zone for a range of incident position angles can be determined by the number of reflection as given in the following equation (El-Refaie, 1989):

$$n^{\text{th}} = [(\theta - \sin^{-1} R)/(\pi - 2\theta)] + 1 \quad (1)$$

where $n^{\text{th}} \geq 1$ and $\sin^{-1} R$ is shadow angle, λ . The consideration of shadow angle due to the shading of receiver can improve the accuracy of the reflection characterisation of the system. Some previous studies have neglected the effect of receiver thickness in estimating the performance of the solar bowl system (Gandhe *et al.*, 1986a; 1986b; 1989). Fig. 2 illustrates the reflection behaviour of the spherical reflector.

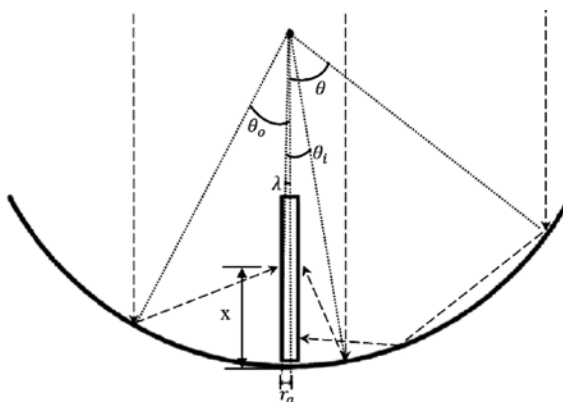


Fig. 2: The optical characteristics of the solar reflector

Solar Receiver Model

Solar receiver is an important component of a solar collector. The incident radiation is reflected and concentrated by a stationary spherical reflector on a certain point along the receiver. The receiver, with a cylindrical shape, is applied in the system. To achieve a more detailed analysis of the receiver, i.e. the term normalised distance, X , was introduced to represent a coordinate along the receiver. X is the ratio of the distance of the reflected rays on the receiver measured from the reflector surface (x) to the radius of reflector (r_s). By referring to the geometry and reflection characteristics of the collector, the normalised distance can be formulated in the form (El-Refaie, 1989):

$$X = \sqrt{(1 - R^2)} + (-1)^n \sin \theta / \sin(2n\theta) - R \cot(2n\theta) \quad (2)$$

The normalised distance is influenced by the diameter ratio of the receiver to reflector and the number of reflection shaped on the reflector. After analysing the range of incident angle for each reflection zone, the corresponding incident angles are substituted in equation (2) to

find the exact point of the reflected radiation on the receiver. The size of the receiver should be appropriate to prevent miss interception of the incoming solar radiation. The minimum diameter ratio that is required to intercept the rays at a particular position angle can be determined using the following equation (El-Refaie, 1989):

$$R \geq \frac{4.65 \times 10^{-3} \sin(2n\theta) \left[(n-1) \frac{\sin(2\theta)}{\sin\theta} + \frac{\sin(2n-1)\theta}{\sin(2n\theta)} \right]}{\sin(2n\theta) - (-1)^n \times 4.65 \times 10^{-3}} \quad (3)$$

Solar Bowl Performance Model

The performance of the UPM Solar Bowl can be predicted by simulating its concentration ratio profile at any particular point, x, along the receiver. Meanwhile, the local concentration ratio can be formulated as follows (El-Refaie, 1989):

$$C_L = \frac{1}{2R} \left\{ \sum_{n=1}^j \rho^n [S(\theta, n) - S(\theta_0, n)] \right\} \quad (4)$$

where,

$$S(\theta, n) = \frac{\sin 2\theta \sin^2(2n\theta)}{(-1)^n [\sin(2n\theta) \cos \theta - 2n \sin \theta \cos(2n\theta)] + 2nR} \quad (5)$$

Equation (4) was derived for the condition in which the outer incident angle of the corresponding number of reflection zone, *j* is less than the rim angle of reflector. This equation was applied to analyse the power concentration ratio when the incident radiation is normal to the aperture of the reflector. Hence, the derivation is merely valid for solar noon. To investigate the system performance in time domain, a theoretical model of the incident solar radiation for the off solar noon hour should be developed. A portion of the stationary solar bowl surface would be shaded for zenith angle, $\xi > 90^\circ - \psi$. According to El-Refaie (1989), a full circumferentially uniform distribution of solar radiation can be reflected on the receiver in the limiting incident angle, $\bar{\theta} = \psi - \xi$. For the incident angle higher than $\bar{\theta}$, there is only a portion of the incident radiation that may be reflected to the receiver. Fig.3 illustrates this particular feature of the bowl during oblique incident case. The sector angle in which no reflection is produced at a particular incident angle is termed as the angle of non-irradiated region, 2ϕ . The section with an included angle of radiation ($2\pi - 2\phi$) will reflect the incident radiation to the receiver. Since the angle of the non-irradiated region for each respective incident angle varies from time to time as the zenith angle changes, the portion of the reflected radiation arriving on the receiver should be identified to determine the average local concentration ratio for the inclined incident radiation. Thus, a mathematical model could be developed to find the angle ϕ , considering the relationship of the functions of elliptical formation, Cartesian coordinates, rim angle, zenith angle and incident angle. After solving the function, the half angle of the non-irradiated region can be written as follows (El-Refaie, 1989):

$$\phi = \tan^{-1} \left\{ \left[(\sin \psi \sin \xi)^2 - (\cos \theta - \cos \psi \cos \xi)^2 \right]^{1/2} / [\cos \xi \cos \theta - \cos \psi] \right\} \quad (6)$$

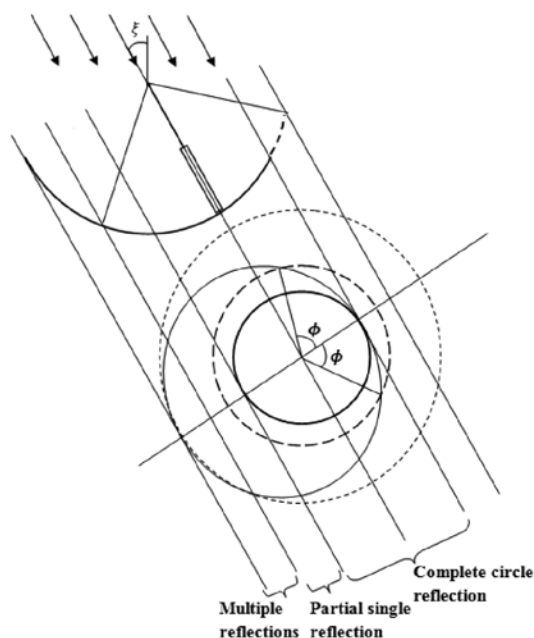


Fig. 3: A projected view on plane normal to incident sunrays for oblique incident investigation (Gandhe *et al.*, 1986a; El-Refaie, 1989; Sulaiman *et al.*, 1997)

A fraction of the incident radiation reflected on the receiver for a particular incident angle can be determined after solving the angle of non-irradiated region of the solar bowl. The fraction of reflected solar flux on the receiver can be defined as:

$$\alpha = 1 - \phi/\pi \quad (7)$$

In the performance analysis of solar bowl during the oblique incident radiation, the analytical model indicated in equation (4) can be applied with modification. Since the mathematical model is derived merely for a complete circle reflection, improvement of the existing model can be introduced considering the partial radiation reflected on the receiver that can provide solution for the off solar noon period. The understanding of the incident angle in affecting solar intensity is important to model the system analysis. The local concentration ratio at a specific location on the receiver with complete circle reflection can be carried out without amending the equation. For the remaining portion of the single reflection (partial single reflection shown in Fig.3), the local power concentration ratio was evaluated separately. The third region of reflection, namely multiple reflections zone, was not taken into consideration in the present work because the multi reflected irradiation might not illuminate the receiver for the absence of lower order of radiation on that point (El-Refaie, 1989; Sulaiman *et al.*, 1997). At the same time, the concentrated energy was assumed to be uniformly absorbed by the receiver circumference on its respective normalised distance. Then, the total concentrated energy for the partial reflection of radiation at a particular location on the receiver could be determined. The average local concentration ratio,

C_L , could be calculated using equation (7), together with equation (5), to predict the local concentration in daytime basis. A proposed equation is introduced as follows:

$$C_L = \frac{1}{2R} \left\{ \sum_{N=1}^J \rho^n [\alpha_{i,S}(\theta_i, n) - \alpha_o, n] \right\} \quad (8)$$

The model presented above was based on the elementary analysis of the incident radiation reflected on reflector surface for all ranges of single reflection (*see* Fig.3). As illustrated in Fig.2, two beam radiations with different incident angles (known as the inner and outer radiations) may arrive at the same normalised distance, x . Thus, the local concentration at a specific coordinate of receiver can be determined by taking into account the different fractions of the reflected solar flux from both the beams on the receiver. The fraction for a particular incident angle, at different zenith angles, can be simulated according to equations (6) and (7). To predict the power concentration, the boundary conditions of the incident angle for complete and partial radiations at different zenith angles should be clearly defined. The boundary conditions of the complete and partial radiation are defined as follows:

- (i) Limit of complete radiation, $\bar{\theta}$: $\lambda < \bar{\theta} \leq \psi - \xi$
 - (ii) Limit of partial radiation, θ_α : $\psi - \xi < \theta_\alpha \leq \psi$
- (9)

Table 2 presents the proposed boundary conditions for both the complete and partial radiations on the receiver.

Table 2: Boundary conditions for complete and partial radiations at different solar time

Solar time	Zenith angle, ξ	Range of complete radiation, $\bar{\theta}$	Range of partial radiation, θ_α
08:00	60	0	$\lambda < \theta_\alpha \leq 60$
09:00	45	$\lambda < \bar{\theta} \leq 15$	$15 < \theta_\alpha \leq 60$
10:00	30	$\lambda < \bar{\theta} \leq 30$	$30 < \theta_\alpha \leq 60$
11:00	15	$\lambda < \bar{\theta} \leq 45$	$45 < \theta_\alpha \leq 60$
12:00	0	$\lambda < \bar{\theta} \leq 60$	0
13:00	15	$\lambda < \bar{\theta} \leq 45$	$45 < \theta_\alpha \leq 60$
14:00	30	$\lambda < \bar{\theta} \leq 30$	$30 < \theta_\alpha \leq 60$
15:00	45	$\lambda < \bar{\theta} \leq 15$	$15 < \theta_\alpha \leq 60$
16:00	60	0	$\lambda < \theta_\alpha \leq 60$

Solar Irradiance Model

In the solar collector analysis, accurate climatic data are needed to obtain a realistic prediction. The actual weather database at the site of UPM Solar Bowl is not available for the present study. Therefore, the estimation of the solar radiation variations at that place during a particular time with tolerable quality was required in the numerical model. Only direct radiation was taken

into account when evaluating the collector performance. Meanwhile, the direct solar radiation intensity on the bowl was assumed to be uniform under a clear sky condition. According to Hottel (1976), the clear day atmospheric transmittance, τ_b , for the beam radiation can be predicted using the following equation:

$$\tau_b = a_0 + a_1 e^{(-k/\cos\xi)} \quad (11)$$

where a_0 , a_1 and k are constants and defined as:

$$\begin{aligned} a_0 &= r_0 \{0.4237 - 0.00821(6 - A)^2\} \\ a_1 &= r_1 \{0.5055 - 0.00595(6.5 - A)^2\} \\ k &= r_k \{0.2711 - 0.01858(2.5 - A)^2\} \end{aligned} \quad (12)$$

where r_0 , r_1 and r_k are the recommended correction factors for different climate zone. From the literature (Hottel, 1976), the values of r_0 , r_1 and r_k for the tropical sky are 0.95, 0.98 and 1.02, respectively. The estimation of the clear sky horizontal direct solar radiation, G_{cb} , can be determined by (Duffie & Beckman, 2006):

$$G_{cb} = G_{on} \tau_b \cos\xi \quad (13)$$

Then, the simulated G_{cb} is associated in the collector simulation model to predict the performance of the solar bowl for a typical day.

NUMERICAL SIMULATION

The simulation of the numerical model was divided into three modules: (i) reflection characterisation of the bowl, (ii) solar flux density along the receiver, and (iii) radiation contours mapping of the receiver. Matlab version R2008a, v7.6.0, was used as a platform to perform the iterative simulation of the UPM Solar Bowl. All the outputs generated by the simulation model are presented in GUI interface. 24-hour notation was used in the function of time. In the study, the incident sunray was assumed normal to the surface of collector at 12:00 solar time and the operating duration of the model system is 8 hours starting from 08:00 to 16:00. The UPM Solar Bowl was modelled under cloudless circumstance in one daytime under the tropical zone. The simulation was conducted on 1st July that is a typical day of clear sky to better estimate its performance (Assilzadeh *et al.*, 2005).

RESULTS AND DISCUSSION

Fig.4 shows the relationship between the number of reflections and the incident angle of radiation. In the UPM Solar Bowl, due to the 60° rim angle, only single reflection was generated when the incoming radiation is normal to the bowl surface. A higher number of reflection was formed as the apparent position of the sun was deviated from the normal axis of the bowl. To quantify the results, Table 3 is tabulated to present the reflection distribution of the bowl up to tenth order of reflection zone. The first order of reflection represents a shadow angle of the model system that the bowl surface forms no reflection within the indicated range (1.01%)

due to the blocking of incident rays by the receiver. The second order of the reflection zone represents a single reflection, whereas the third zone is for double reflection and so forth. The simulated result shows that the single reflection covers the largest range of incident angle up to 69.66%. Meanwhile, the multiple reflections appear for a relatively small range and keep reducing at the higher order of reflection zone.

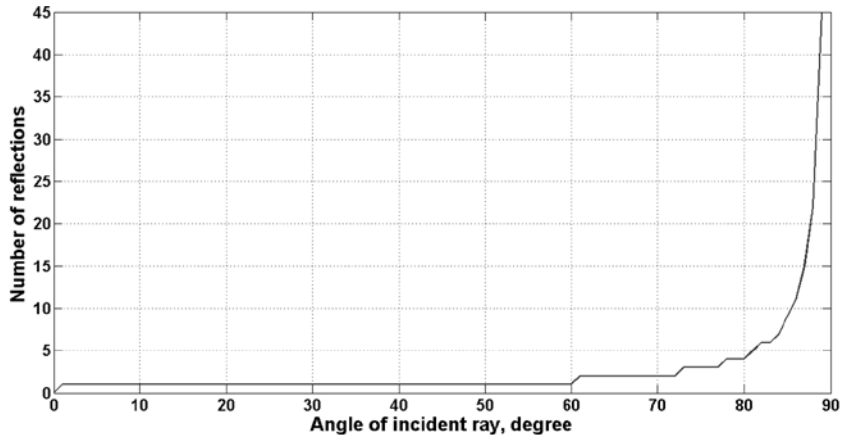


Fig. 4: Multiple reflection characteristics in various angles of the incident rays

Table 3: Reflection distribution of the solar bowl

Order of reflection zone (n^{th})	Number of reflection (n)	Range of incident angle (degree)	Percentage of the range of incident angle (%)
First	Non (λ)	$0 \leq \theta < 0.859$	1.01
Second	1	$0.859 \leq \theta < 60.286$	69.66
Third	2	$60.286 \leq \theta < 72.172$	13.93
Fourth	3	$72.172 \leq \theta < 77.266$	5.97
Fifth	4	$77.266 \leq \theta < 80.095$	3.32
Sixth	5	$80.095 \leq \theta < 81.896$	2.11
Seventh	6	$81.896 \leq \theta < 83.143$	1.46
Eight	7	$83.143 \leq \theta < 84.057$	1.07
Ninth	8	$84.057 \leq \theta < 84.756$	0.82
Tenth	9	$84.756 \leq \theta < 85.308$	0.65

The range of incident ray varies throughout the daytime due to the apparent movement of the sun position relative to the earth surface. Fig.5 indicates the maximum incident angles and their respective number of reflections in the function of time. The maximum angle of the incident on the reflector is 90° at 08:00. After two hours, the maximum incident angle begins to decrease linearly until 60° at solar noon. The plots of the results are symmetrical at the daytime axis at 12:00 because of the assumed symmetry property of spherical reflector and the consistent apparent motion of the sun passing through the bowl centre.

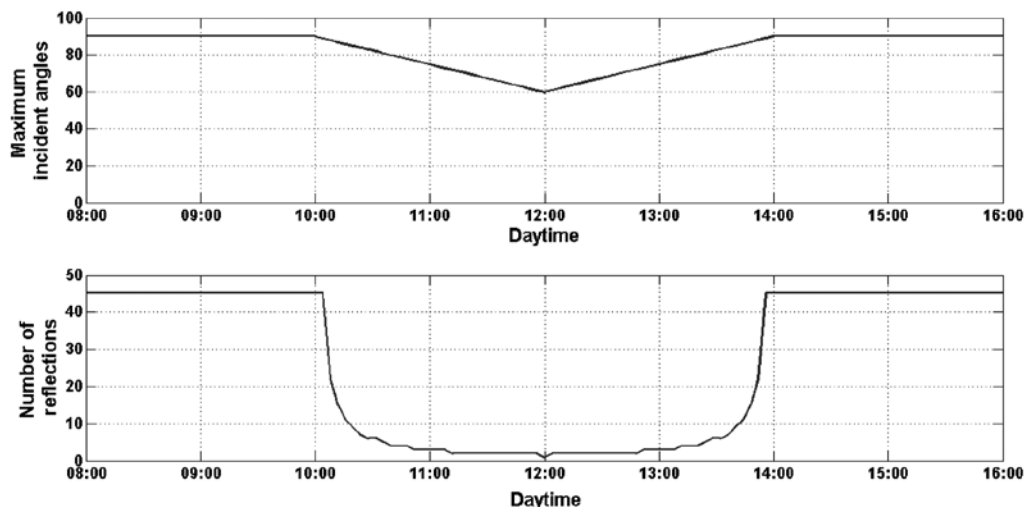


Fig. 5: The maximum incident angles and the number of reflections on the UPM Solar Bowl reflector in one daytime

The reflected solar radiation on a specific coordinate of the cylindrical receiver is shown in Fig.6. The normalised distance result shows a similar shape of plot as compared to the published data that used different quantities of geometry size (El-Refair, 1989; Sulaiman *et al.*, 1997). As presented in the figure, the single reflection intercepts the receiver from normalised distances 0 to 0.456 which is equivalent to the actual distance extending from the bowl surface to 12.72 m above it. Nevertheless, there is no incident radiation striking the receiver at normalised distance more than 0.456. Thus, the length of the receiver may not need be extended beyond that point. Fig.7 shows the distance coverage of the receiver which is illuminated by the different numbers of reflection. The coverage region of the reflected ray on the receiver is relatively small for higher reflection zone. This result is important in defining the appropriate length of receiver in the system.

From the information presented in Fig.6 and Fig.7, the multiple reflections may not contribute to the solar energy concentration on the receiver with a normalised distance more than 0.0798 or 2.23 m from the bowl surface. In the model, the length of the receiver was designed to have normalised distance from 0.10 to 0.45. This means the receiver is illuminated by the single radiation only. Thus, the performance evaluation of the UPM Solar Bowl, based on the single reflection zone, is tolerable in determining the collector performance due to the dimension constraint of the receiver. In addition, the optical property of the multiple reflections is uncontrollable and suffering successive losses in efficiency. Fig.8 presents the required minimum diameter of the receiver for a complete interception of the reflected radiation. From this result, it was found that the size of the receiver model is able to intercept all the incoming solar radiations up to the tenth order of the reflection zone. This information is useful to optimise the size of the receiver for the UPM Solar Bowl.

Fig.9 shows the concentration ratio on different normalised distances for incident radiation normal to the reflector's aperture. The simulation result reports that the concentrated solar

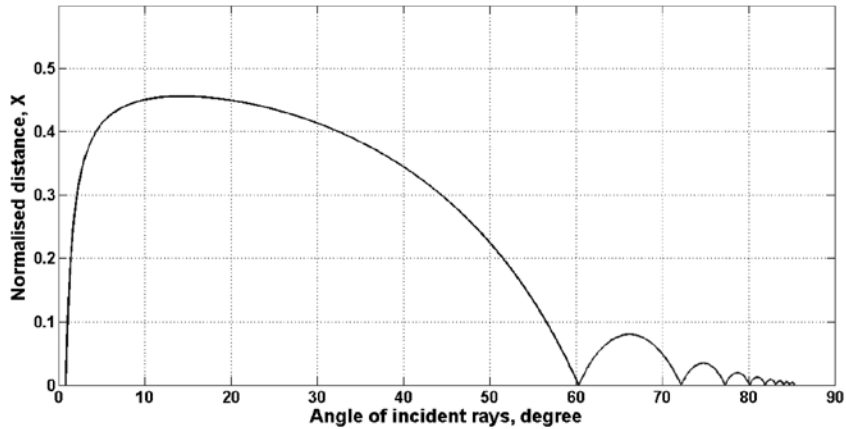


Fig. 6: Normalised distance X against position angle for R=0.015

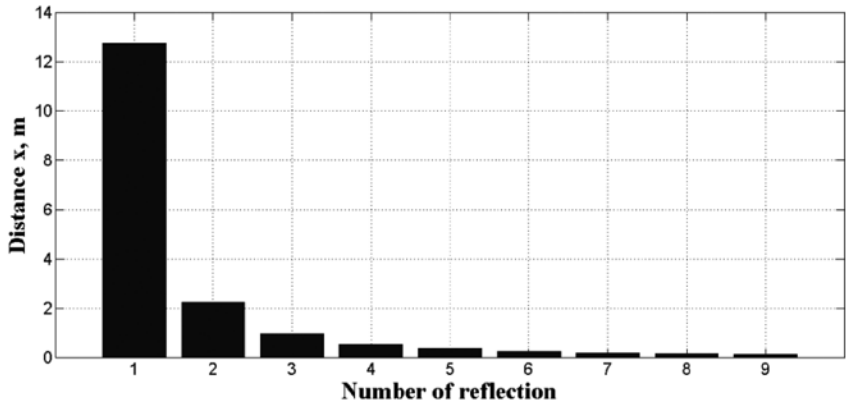


Fig. 7: The range of the distance x on receiver that can receive incident radiation for the different numbers of reflection

irradiation is the highest at the upper part of the receiver and it gradually decreases towards the lower portion of the receiver.

The effect of the angular deviation of incident radiation on the solar bowl due to the apparent motion of the sun is presented in this paper. The fractions of the reflected solar radiation, with continuous incident angles for different zenith angles, are shown in Fig.10. It is obvious that a high zenith angle induces to a relatively low level proportion of the reflected solar flux on the receiver due to the larger cosine loss. As an example, the incident angle of 45°, 100% of the reflected solar flux at this incident angle can reach the receiver at 10° zenith angle, 73.8% at 20° zenith angle, 60.3% at 30° zenith angle, 52.9% at 40° zenith angle, 47.3% at 50° zenith angle and 42.3% at 60° zenith angle.

Fig.11 reports the overall concentration ratio along the receiver in the time domain. The collector concentration ratio varies with the functions of time and normalised distances of the receiver. A higher normalised distance is competent to collect more thermal energy for longer

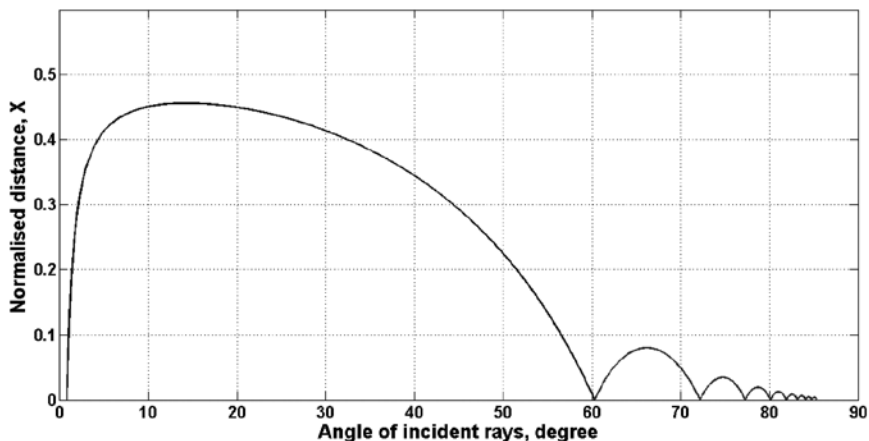


Fig. 8: The minimum size of the receiver for radiation interception

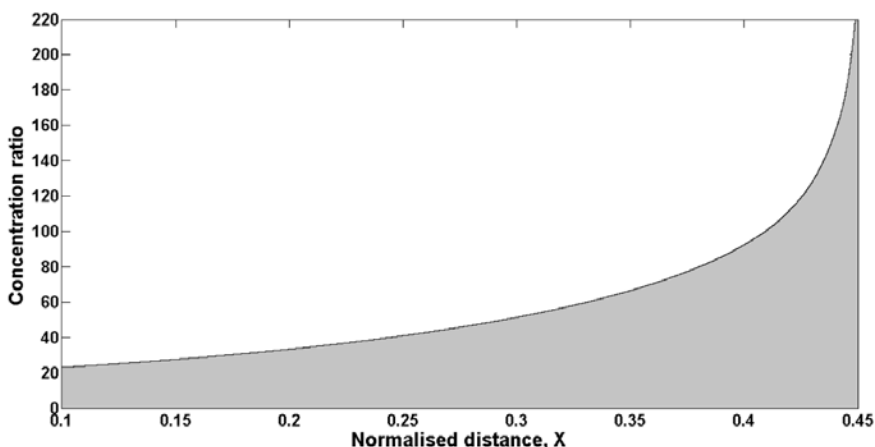


Fig. 9: Concentration ratio along the receiver for normal incident case

period. At 0.44 normalised distance, the concentration ratio is 73 at 08:00 and it increases to 156 after two hours (113.7% increment). The power concentration is then constant for four hours until 14:00 and reducing to 73 at 16:00. On the contrary, the concentration ratio deteriorates substantially during the off solar noon hour. Similar trend profiles were also observed at the lower normalised distances of the receiver.

Fig.12 shows the simulated profile of the solar flux density of the bowl at different normalised distances on 1st July 2010 under the assumed clear sky of tropic. This simulation result was compared to the experimental data from the literature, as in Gandhe *et al.* (1989) and Dirks *et al.* (1992) who had presented thermal performance and collector efficiency respectively in daytime. These comparisons indicated a fair similar shape of curve. According to the result, the maximum solar flux density is 119.1 kW/m², as can be seen at 0.44 normalised distance during 12:00. At 08:00 and 16:00, the flux concentration at the same coordinate is only 20.95 kW/m², which is equivalent to the 82.4% reduction of solar flux energy. Table 4

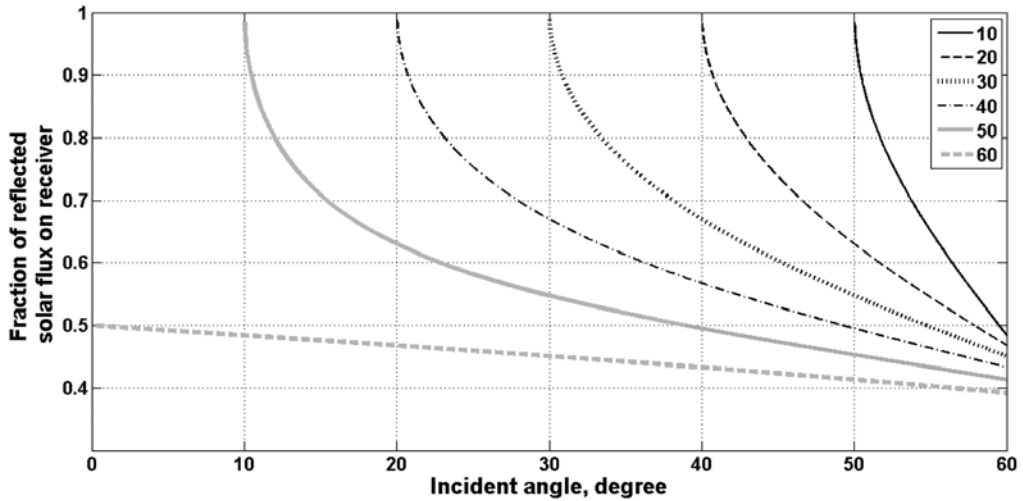


Fig. 10: Fractions of the available reflected solar radiation with respective incident angles for different zenith angles

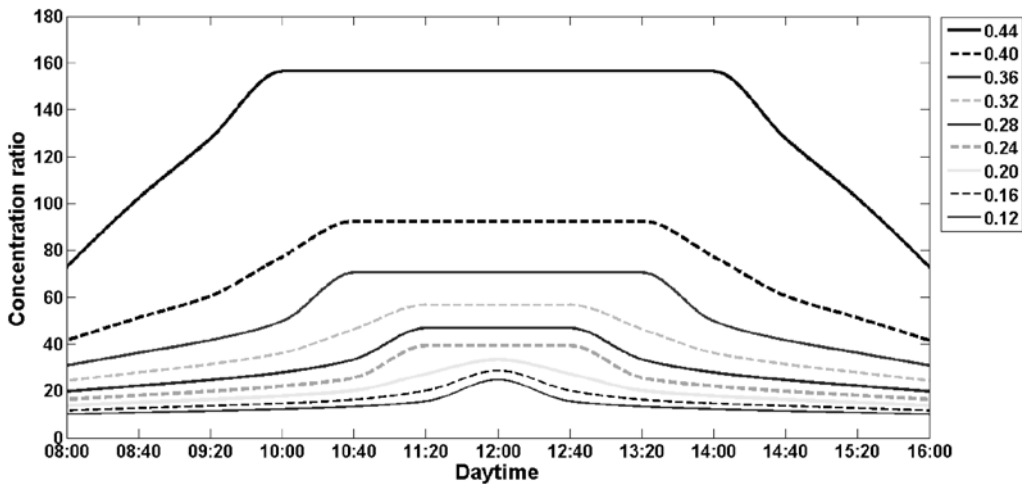


Fig. 11: Estimated concentration ratio at different normalised distances on the receiver in daytime

reports the calculated percentage of reduction of flux density with respect to each individual maximum flux concentration, at different normalised distances along the receiver for the off solar noon hour. This table shows the performance deterioration of the solar bowl. Based on the information presented in Table 4, at the higher region of receiver (normalised distances of 0.44, 0.40 and 0.36), the available solar flux density drops to less than 7.8% within 80 minutes from the solar noon in cloudless sky. It can be noted that the concentrated solar energy at the lower region decreases in a relatively higher rate. The performance of the bowl at a high zenith angle appears to be very undesirable in which the percentage reduction of the flux density is more than 82% at all points of the receiver during 08:00 and 16:00.

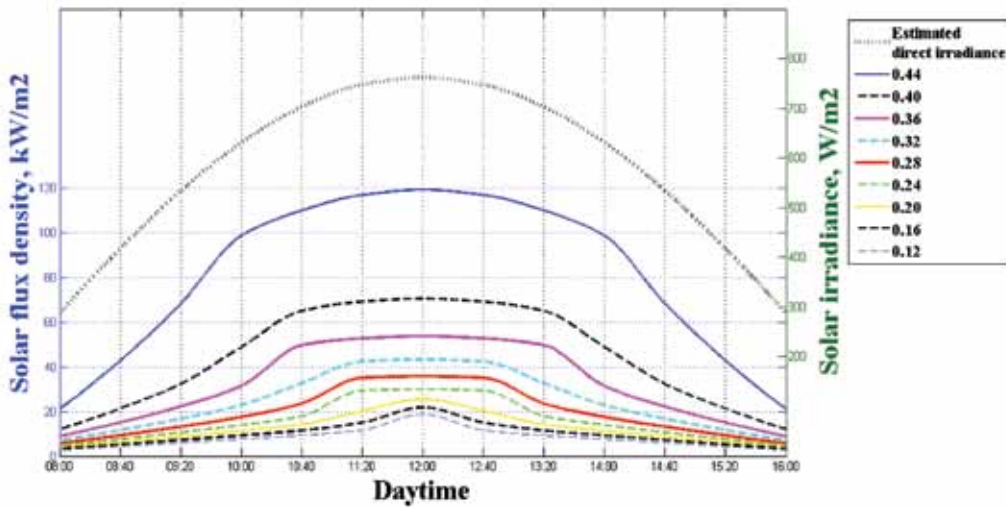


Fig. 12: Solar flux density of the UPM Solar Bowl at different normalised distances on 1st July 2010 under the tropical clear sky condition

Table 4: The percentage of reduction (%) of the solar flux density on the receiver

Solar time	Normalised distance								
	0.12	0.16	0.20	0.24	0.28	0.32	0.36	0.40	0.44
08:00/ 16:00	84.8	84.6	84.5	84.3	84.1	83.8	83.5	83.0	82.4
08:40/ 15:20	76.4	75.9	75.4	74.8	74.1	73.2	71.9	69.8	64.2
09:20/ 14:40	67.7	66.9	65.8	64.6	63.2	61.3	58.6	54.2	42.8
10:00/ 14:00	59.2	57.7	55.8	53.6	50.9	47.2	41.7	30.9	17.3
10:40/ 13:20	50.6	47.7	44.3	40.6	34.2	24.9	7.8	7.8	7.8
11:20/ 12:40	38.3	31.1	20.2	1.9	2.0	2.0	2.0	2.0	2.0

The radiation contour mapping of the receiver is essential to identify the illumination characterisation. There are three types of illumination regions on the receiver, and these are known as completely irradiated region, partially irradiated region and non-irradiated region. Fig.13 presents the receiver contour mapping of UPM Solar Bowl. It shows a similar trend of radiation contour mapping to that of El-Refaie (1989) and Sulaiman *et al.* (1997) which have been analysed at different sizes of collector. At the angular deviation 0°, the entire surface area of receiver is completely irradiated. The partially irradiated region, which is also known as the faintly-irradiated region, starts to grow gradually for non-normal incident radiation as can be seen in the angular deviations of 10°, 20°, 30°, 40°, 50° and 52°. For the angular deviation greater than 50°, the partially irradiated region occupies more than 50% of the surface area of the receiver. From this simulation result, it can be observed that in a higher angular deviation, non-irradiated region begins to emerge and expand progressively as shown at the angular deviation of 54°, 56°, 58° and 60°. It is crucial to note that about half of the receiver region is unirradiated at angular deviation 60°. This result agrees to the finding discussed by Bar-Lev *et al.* (1983), in which for their solar bowl system, there was only about 50% of the illuminated

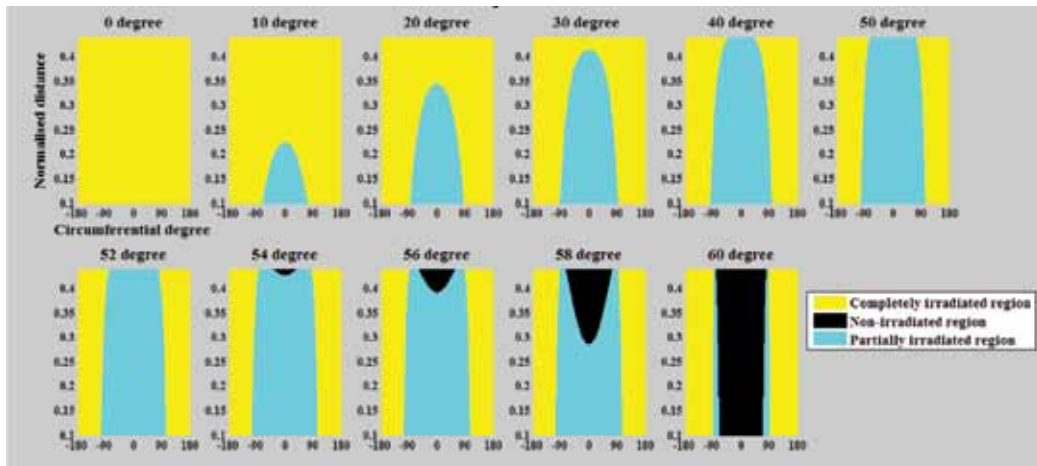


Fig. 13: The contour of completely, partially and non-irradiated region on receiver

receiver area covered with solar cells considering the worst case at 08:00 and 16:00. This contour mapping explains the reason for the substantial low solar concentration power during high solar zenith angle.

CONCLUSIONS

A numerical simulation model of the UPM Solar Bowl was developed in this study. Reflection characterisation and performance models of the bowl in tropics were successfully assessed in the Matlab simulation platform, which can predict and quantify the results in time domain. The present work can advance the understanding of the fundamental aspects of the solar bowl and be used to achieve useful information on the plant performance. Any further investigation may focus on the experimental study of the solar collector under the real meteorological environment in the tropical area. Thus, a reliable solar harnessing technology and innovative collector design to improve the collector performance should be developed to assess the possibilities of solar bowl power system in the future.

REFERENCES

- Assilzadeh, F., Kalogirou, S. A., Ali, Y., & Sopian, K. (2005). Simulation and optimization of a LiBr solar absorption cooling system with evacuated tube collectors. *Renewable Energy*, 30(8), 1143-1159.
- Bar-Lev, A., Waks, S., & Grossman, G. (1983). Analysis of a Combined Thermal-Photovoltaic Solar System Based on the Spherical Reflector/Tracking Absorber Concentrator. *Journal of Solar Energy Engineering*, 105(3), 322-328.
- Bethea, R. M., Barriger, M. T., Williams, P. F., & Chin, S. (1981). Environmental effects on solar concentrator mirrors. *Solar Energy*, 27(6), 497-511.
- Clausing, A. M. (1976). The performance of a stationary reflector/ tracking absorber solar concentrator. In K. W. Boer (Ed.), *Sharing the Sun - Solar Technology in the Seventies* (Vol. 2): The American Section of the International Solar Energy Society.

- Dirks, J. A., Williams, T. A., & Brown, D. R. (1992). Performance and Cost Implications of the Fixed Mirror, Distributed Focus (FMDF) Collector. *Journal of Solar Energy Engineering*, 114(4), 254-259.
- Duffie, J. A., & Beckman, W. A. (2006). *Solar Engineering of Thermal Processes* (3rd ed.). United States of America: John Wiley & Sons, Inc.
- El-Refaie, M. F. (1989). Performance analysis of the stationary-reflector/tracking-absorber solar collector. *Energy Conversion and Management*, 29(2), 111-127.
- Gandhe, V. B., Venkatesh, A., & Sriramulu, V. (1986a). Analysis of a fixed spherical reflector exposed to oblique incident rays. *Energy Conversion and Management*, 26(3-4), 363-368.
- Gandhe, V. B., Venkatesh, A., & Sriramulu, V. (1986b). Optical analysis of a cylindrical absorber in a fixed spherical reflector. *Energy*, 11(10), 969-976.
- Gandhe, V. B., Venkatesh, A., & Sriramulu, V. (1989). Thermal analysis of an FMDF solar concentrator. *Solar & Wind Technology*, 6(3), 197-202.
- Garcia-Valladares, O., & Velazquez, N. (2009). Numerical simulation of parabolic trough solar collector: Improvement using counter flow concentric circular heat exchangers. *International Journal of Heat and Mass Transfer*, 52(3-4), 597-609.
- Hottel, H. C. (1976). A simple model for estimating the transmittance of direct solar radiation through clear atmospheres. *Solar Energy*, 18(2), 129-134.
- Kreider, J. F. (1975). Thermal Performance Analysis of the Stationary Reflector/Tracking Absorber (SRTA) Solar Concentrator. *Journal of Heat Transfer*, 97(3), 451-456.
- O'Hair, E. A., & Green, B. L. (1990). *Component Efficiencies From The Operation Of The Crosbyton Solar Bowl*. Paper presented at the Energy Conversion Engineering Conference, 1990. IECEC-90. Proceedings of the 25th Intersociety.
- O'Hair, E. A., & Green, B. L. (1992). Solar Bowl Component Efficiencies. *Journal of Solar Energy Engineering*, 114(4), 272-274.
- Sulaiman, M. Y., Bashria, A. Y., Ali, M., & Adam, N. M. (2008). *Design of tracking system for UPM solar bowl*. Paper presented at the Proceeding of Seminar on Progress of Solar Energy Research and Development.
- Sulaiman, M. Y., Hlaing Oo, W. M., Wahab, M. A., Sulaiman, Z. A., & Khouzam, K. Y. (1997). Conceptual design of a hybrid thermal and photovoltaic receiver of an FMDF collector. *Renewable Energy*, 12(1), 91-98.